Generation of Maximally Entangled Long-Lived States with Giant Atoms in a Waveguide

Alan C. Santos[1,2,*] and R. Bachelard[1,3,†]

[1]*Departamento de Física, Universidade Federal de São Carlos, Rodovia Washington Luís, km 235—SP-310, 13565-905 São Carlos, São Paulo, Brazil*

[2]*Department of Physics, Stockholm University, AlbaNova University Center, 106 91 Stockholm, Sweden*

[3]*Université Côte d'Azur, CNRS, Institut de Physique de Nice, 06560 Valbonne, France*

(Received 21 July 2022; revised 28 October 2022; accepted 11 January 2023; published 1 February 2023)

In this Letter, we show how to efficiently generate entanglement between two artificial giant atoms with photon-mediated interactions in a waveguide. Taking advantage of the adjustable decay processes of giant atoms into the waveguide and of the interference processes, spontaneous sudden birth of entanglement can be strongly enhanced with giant atoms. Highly entangled states can also be generated in the steady-state regime when the system is driven by a resonant classical field. We show that the statistics of the light emitted by the system can be used as a witness of the presence of entanglement in the system, since giant photon bunching is observed close to the regime of maximal entanglement. Given the degree of quantum correlations incoherently generated in this system, our results open a broad avenue for the generation of quantum correlations and manipulation of photon statistics in systems of giant atoms.

DOI: 10.1103/PhysRevLett.130.053601

Artificial atoms in a waveguide constitute the heart of superconducting quantum circuits [1], with the photon-mediated interaction between distant atoms leading to collective effects such as sub- and superradiance [2,3], and allow for the creation and transport of strongly correlated photons [4,5]. Such systems have been used to create maximally entangled states of N two-level atoms [6], which are important resources for quantum information [7,8] and communication [9,10], for example. However, maintaining this entanglement over time is all the more challenging because of decoherence processes. This has led to the development of strategies to harness this decoherence and generate entanglement between subsystems, for instance, by coupling the system to thermal baths of negative temperature [11] or fermionic reservoirs [12], by exploiting memory effects of the environment [13], or through the coherent control of nondegenerate atoms in cavities [14].

Identifying configurations where the effect of the environment on the entanglement is reduced to its minimum is an important task for the development of quantum technologies. In the frame of waveguide quantum electrodynamics, a promising alternative to small emitters has been introduced: "giant atoms" are emitters whose coupling with a guided wave extends over such a length that their interaction cannot be described as that of pointlike emitters [15,16]. In particular, the dipole approximation does not hold any longer [17–19]. The peculiar characteristics of giant atoms, such as frequency-dependent relaxation rates [15,20–23] and decoherence-free mediated interaction between two atoms [24,25], make this system an ideal platform for the robust generation of entanglement [26,27]. The multiple connections between each atom and the waveguide, and the possibility to intertwine the different atoms through their connection points, opens a broad field of perspectives for the manipulation of entangled states and for information processing, which has barely been scratched up to now [16].

We study entanglement generation for two giant atoms through nonunitary (incoherent) decay processes. More specifically, we show how two giant atoms interacting with a waveguide, sketched in Fig. 1(a), can be used to create, control, and engineer metastable entangled states. Adjusting the frequency ω_0 of the light in the waveguide, we are able to tune the asymmetry of the decay rates in different decay channels, as shown in Fig. 1(b). We take advantage of this property to stimulate the sudden birth of concurrence, generating quantum correlations 1 order of magnitude larger than for small atoms. In addition, adjusting the external control field and the frequency ω_0, we show how long-lived entangled states can be efficiently created through a strategy of population inversion in the steady state [Figs. 1(c) and 1(d)]. Different from previous studies, our scheme does not require reservoir engineering [11,12], non-Markovian effects [13], or energy level engineering [14]: the unique properties of giant atoms in terms of decoherence and energy levels are exploited to prepare maximally entangled steady states. Finally, we show that the statistics of the light emitted by the atoms in the waveguide can be used as an entanglement witness in the system, so the entanglement can be monitored in a nondestructive way through the scattered light.

Coupled dynamics of giant atoms.—We consider N giant two-level atoms interacting with a one-dimensional waveguide. Atom k is coupled to the waveguide in K_k points, at positions $\{x_n^{(k)}\}$ with decay rate $\gamma_n^{(k)}$ (with $k = \{1, \ldots, N\}$ and $n = \{1, \ldots, K_k\}$). In the weak coupling limit and rotating wave approximation, the effective dynamics of the atoms is described by a density matrix $\hat{\rho}$ obtained by tracing out the bosonic modes of the waveguide [15,24],

$$\frac{d}{dt}\hat{\rho}(t) = \frac{1}{i\hbar}[\hat{H}_0 + \hat{H}_{\mathrm{cc}}, \hat{\rho}(t)] + \mathcal{L}[\hat{\rho}(t)], \tag{1}$$

with $\hat{H}_0 = \sum_{n=1}^{N} \hbar(\omega_n + \delta_n)\hat{\sigma}_n^+\hat{\sigma}_n^-$ the Hamiltonian of the independent atoms. The frequency shift $\delta_k = (1/2)\sum_{\ell=1}^{K_k}\sum_{m=1}^{K_k}(\gamma_\ell^{(k)}\gamma_m^{(k)})^{1/2}\sin\varphi_{\ell,m}^{k,k}$ of each atom stems from the phase $\varphi_{\ell,m}^{k,n} = \kappa|x_\ell^{(k)} - x_m^{(n)}|$ acquired by the wave as it propagates between the connection points $x_\ell^{(k)}$ and $x_m^{(n)}$, where κ is the wave number of the light in the waveguide. Atom-atom interaction is composed of a coherent excitation-exchange component $\hat{H}_{\mathrm{cc}} = \hbar\sum_{j\neq n}^{N}\sum_{n=1}^{N}\Delta_{jn}\hat{\sigma}_j^+\hat{\sigma}_n^-$, with $\Delta_{jn} = (1/2)\sum_\ell^{K_j}\sum_m^{K_n}(\gamma_\ell^{(j)}\gamma_m^{(n)})^{1/2}\sin\varphi_{\ell,m}^{j,n}$, and a dissipative part given by the Lindbladian,

$$\mathcal{L}[\hat{\rho}(t)] = \frac{1}{2}\sum_{j,n=1}^{N,N}\Gamma_{jn}[2\hat{\sigma}_j^-\hat{\rho}(t)\hat{\sigma}_n^+ - \{\hat{\sigma}_j^+\hat{\sigma}_n^-, \hat{\rho}(t)\}], \tag{2}$$

with $\Gamma_{jn} = \sum_\ell^{K_j}\sum_m^{K_n}(\gamma_\ell^{(j)}\gamma_m^{(n)})^{1/2}\cos\varphi_{\ell,m}^{j,n}$ the cross decay term. $\Gamma_{jj} = \Gamma_j$ corresponds to the single-atom decay rate. Different from small atoms, this rate depends on the relative phase between the connection points of the given atom, and it is not simply the sum of the decay rate at each connection point of that atom. The atoms are driven by external fields, which add the extra Hamiltonian term (in the rotating frame): $\hat{H}_{\mathrm{ext}} = \hbar\sum_{n=1}^{2}\Omega_0(\hat{\sigma}_n^+ + \hat{\sigma}_n^-)$, with Ω_0 the Rabi frequency of this pump. In superconducting qubits, it can be done with independent drive lines applied to the atoms [28,29], for instance, in which case the Lindblad form of Eq. (1) does not change (see Supplemental Material [30]). The above equations are κ periodic, meaning that retardation effects associated with the propagation time of photons in the waveguide are not accounted for. Non-Markovian dynamics [35–37] can lead to disentanglement and entanglement revival [38,39], yet only when the propagation time becomes $t \sim 1/\gamma_0$. In recent experiments [26], this corresponds to meter-size waveguides.

We focus on the case of two giant atoms with identical frequencies $\omega_n = \omega$ and relaxation rates $\gamma_m^{(n)} = \gamma_0$, connected to the waveguide at two points ($K_1 = K_2 = 2$). The spacing between all neighboring connection points is the same, hereafter called Δx. Figure 1(a) depicts the nested configuration, where the two connections of one atom fall in between the connections of the other. The waveguide-mediated atom-atom interaction results in a shift of the energy levels, which is illustrated in Fig. 1(b). The energy of the different levels is $E_g = 0$, $E_e = \hbar(\tilde{\omega}_1 + \tilde{\omega}_2)$, $E_\pm = \hbar(\tilde{\omega}_1 + \tilde{\omega}_2 \pm \tilde{\Delta})/2$, with $\tilde{\Delta} = \sqrt{4\Delta_{12}^2 + (\tilde{\omega}_1 - \tilde{\omega}_2)^2}$, which are associated with the states $|gg\rangle$, $|ee\rangle$, and

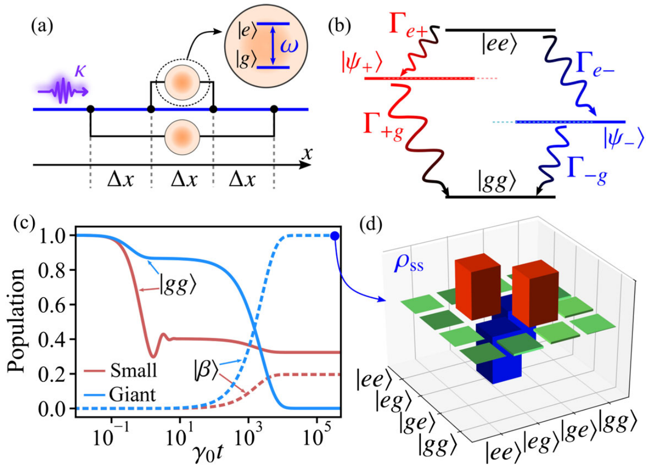

FIG. 1. (a) Two giant atoms in the "nested" configuration considered in the present Letter. (b) Energy diagram showing collective states of the system and the decay rates between them. (c) Population dynamics of the ground state $|gg\rangle$ and the Bell state $|\beta\rangle = (|ge\rangle - |eg\rangle)/\sqrt{2}$, for the nested giant atoms with $\kappa\Delta x/\pi = 0.01$ and Rabi frequency of the external field $\Omega_0 = 1.5\gamma_0$. (d) State tomography of the steady-state density matrix $\rho_{\mathrm{SS}} \approx |\beta\rangle\langle\beta|$ for the dynamics considered in (c).

$$|\psi_\pm\rangle = \frac{1}{\mathcal{N}_\pm}\left[\frac{\tilde{\omega}_1 - \tilde{\omega}_2 \pm \tilde{\Delta}}{\Delta_{12}}|eg\rangle + 2|ge\rangle\right], \tag{3}$$

respectively, where $\mathcal{N}_\pm^2 = 4 + (\tilde{\omega}_1 - \tilde{\omega}_2 \pm \tilde{\Delta})^2/\Delta_{12}^2$ and $\tilde{\omega}_n = \omega + \delta_n$. The eigenstates $|\psi_\pm\rangle$ are single-excitation (entangled) states, with an energy difference $\tilde{\Delta}$. The transition rates between these levels are given by [30]

$$\Gamma_{e+} = \frac{\Gamma_2\eta_+ - \Gamma_1\eta_- + \xi}{2\tilde{\Delta}}, \qquad \Gamma_{+g} = \frac{\Gamma_1\eta_+ - \Gamma_2\eta_- + \xi}{2\tilde{\Delta}}, \tag{4a}$$

$$\Gamma_{e-} = \frac{\Gamma_1\eta_+ - \Gamma_2\eta_- - \xi}{2\tilde{\Delta}}, \qquad \Gamma_{-g} = \frac{\Gamma_2\eta_+ - \Gamma_1\eta_- - \xi}{2\tilde{\Delta}}, \tag{4b}$$

with $\eta_\pm = \tilde{\omega}_1 - \tilde{\omega}_2 \pm \tilde{\Delta}$ and $\xi = 4\Delta_{12}\Gamma_{12}$. Figure 2 shows the behavior of each decay rate for the nested giant atoms and small ones as function of Δx.

For small atoms, the shift δ_n vanishes and all single-atom decay rates are the same: $\Gamma_1 = \Gamma_2$. The shift is then $\tilde{\Delta} = 2|\Gamma_{12}|$, and one obtains that each decay branch (that is, passing either through $|\psi_+\rangle$ or $|\psi_-\rangle$) possesses a single

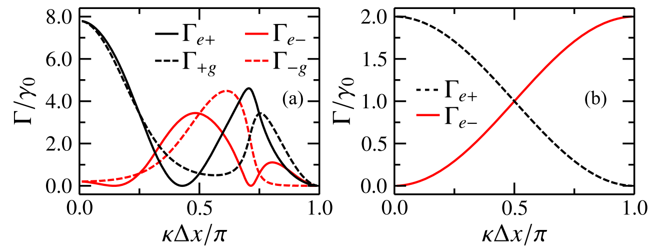

FIG. 2. Collective decay rates, as a function of $\kappa\Delta x$, for (a) two nested giant atoms and (b) two small atoms. For small atoms, one has $\Gamma_{e+} = \Gamma_{+g}$ and $\Gamma_{e-} = \Gamma_{-g}$ for any $\kappa\Delta x$.

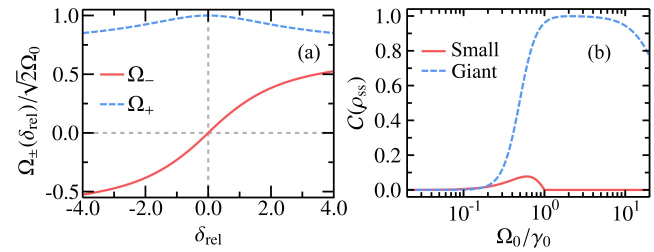

FIG. 3. (a) Effective coupling as function of the relative energy shift $\delta_{\rm rel}$ for nested giant atoms, written as a multiple of $\sqrt{2}\Omega_0$. (b) Steady-state entanglement obtained through local (resonant) fields driving two nested giant atoms, for $\kappa\Delta x = 0.01\pi$.

decay rate: $\Gamma_{e\pm} = \Gamma_{\pm g} = \Gamma_2 \pm \Gamma_{12}\Delta_{12}/|\Delta_{12}|$. In this case, $|\psi_\pm\rangle$ are simply the symmetric and antisymmetric states [40,41]. Differently, for giant atoms, even when the decay rates of all connection points are equal, $\gamma_n^{(k)} = \gamma_0$, the single-atom decay rates are different for each atom ($\Gamma_1 \neq \Gamma_2$) since the relative phases between their connection points are different. Furthermore, the four-level energy structure is characterized by four distinct decay rates, whereas in the case of small atoms, there are only two distinct decay rates. This complex internal structure of the two-giant-atom system leads to new regimes that cannot be reached for small atoms.

Maximally entangled steady state.—Generating stationary entanglement with small atoms coupled to common radiation modes can be achieved using energy shifts, either mediated by the interactions [42–44] or between the raw transition frequencies of the emitters [14]. For giant atoms, the energy shifts are modest ($\tilde{\Delta} \leq 4\gamma_0$), yet the distinct decay rates that connect the $|\psi_\pm\rangle$ states to the fundamental and fully excited state allow one to generate highly entangled stationary states.

In fact, let us consider two atoms initially in the ground state. Figure 1(c) shows the dynamics of the populations of states $|gg\rangle$ and $|\beta\rangle = (|ge\rangle - |eg\rangle)/\sqrt{2}$ for small and giant atoms separated by a distance $\kappa\Delta x = 0.01\pi$. For giant atoms, although the energy shifts are negligible ($\tilde{\Delta} \approx 2\sqrt{10}\gamma_0\kappa\Delta x \ll \gamma_0$), the system reaches a steady state where almost all the population in the state $|\beta\rangle$, with a long lifetime $1/\Gamma_- \approx 546/\gamma_0$ (see Supplemental Material [30]). This highly entangled steady state is represented as a density matrix in Fig. 1(d), where the population is concentrated on the single-excitation sector. Oppositely, for small atoms the system is driven toward a superposition of different states, including the ground state, and it does not become entangled.

Entanglement is quantified by the concurrence of the state, as proposed by Hill and Wootters [45]. The maximally entangled state $|\beta\rangle$ introduced above reaches the value $\mathcal{C}(\rho) = 1$, whereas it is zero for nonentangled states [46]. In the particular case discussed above, see Figs. 1(c) and 1(d), giant atoms present a concurrence of $\mathcal{C} = 0.995$ in the steady-state, while it is precisely $\mathcal{C} = 0$ for small atoms.

Now we discuss the mechanism behind the efficient generation of steady-state entanglement. The efficient coupling of the external field with the atomic transition $|gg\rangle \to |\psi_-\rangle$ plays an important role in this process. The coupling induced by the driving field between the ground state and $|\psi_\pm\rangle$ can be obtained by rewriting the pump term $H_{\rm ext} = \hbar(\Omega_+\hat{\sigma}_+^\dagger + \Omega_-\hat{\sigma}_-^\dagger) + \text{H.c.}$, with $\hat{\sigma}_\pm^\dagger = |\psi_\pm\rangle\langle gg|$, with effective coupling coefficients

$$\Omega_\pm = \Omega_0\left(\frac{\delta_{12} + 2\Delta_{12} \pm \sqrt{4\Delta_{12}^2 + \delta_{12}^2}}{\sqrt{8\Delta_{12}^2 + 2\delta_{12}(\delta_{12} \pm \sqrt{4\Delta_{12}^2 + \delta_{12}^2})}}\right), \quad (5)$$

with $\delta_{12} = \delta_1 - \delta_2$. For small atoms, the driving field allows for population transfer from $|gg\rangle$ to $|ee\rangle$ through the state $|\psi_+\rangle$ at a rate Ω_+. However, we highlight the effective coupling value of Ω_-, which leads to a direct coherent coupling of the transition from the state $|gg\rangle$ to $|\psi_-\rangle$. From the relative phase shift $\delta_{\rm rel} = \delta_{12}/\Delta_{12}$, we get $\Omega_- \neq 0$ for $\delta_{\rm rel} \neq 0$ [see Fig. 3(a)]. In particular, whenever $\delta_1 = \delta_2$, we get $\Omega_- = 0$ and $\Omega_+ = \sqrt{2}\Omega_0$, as observed for small atoms. In this sense, the difference in resonant energy of the atoms due to their finite size induces an efficient coupling to the $|\psi_-\rangle$ state.

This mechanism alone is not enough to get a large population in the state $|\psi_-\rangle$, since a nonzero coupling between $|gg\rangle$ and $|\psi_-\rangle$ also can be achieved for small atoms with different frequencies ω_1 and ω_2 [30]. The interference between the contributions of the states $|\psi_\pm\rangle$ in the steady state needs also to be taken into account, since the steady state $|\beta\rangle$ can be written as superposition of these two states. Steady-state entanglement is optimized when the pump is strong enough for a single-excitation state to be fully populated, yet not enough to populate all the state in the system. The concurrence [Fig. 3(b)] reaches its maximum when the external pump has a Rabi frequency $\Omega_0 \approx 2\gamma_0$. While maximally entangled states are not possible with same-energy small atoms, with a maximum value $\max_{\Omega_0}[\mathcal{C}(\rho_{\rm SS}^{\rm small})] < 0.1$, giant atoms allow one to achieve highly entangled states, with concurrence of order of $\mathcal{C}(\rho_{\rm SS}^{\rm nested}) \approx 0.999$. As one can prepare any of the other Bell states from $|\beta\rangle$ by single-atom (local) operations [46], the steady-state approach proposed in this Letter can be useful to create an arbitrary entangled state of two giant atoms.

Sudden birth of entanglement.—We consider an initially fully inverted state $|ee\rangle$, prepared through a fast π pulse on the atoms. We then let the system decay, in the absence of pump field, monitoring how the action of collective spontaneous emission through sub- and superradiant branches $|\psi_\pm\rangle$ allows one to efficiently generate entanglement. The system first decays toward a mixture of the $|\psi_+\rangle$ and $|\psi_-\rangle$ states, which is in general not entangled, although each of these states is individually entangled. However, because of the difference in their lifetimes $1/\Gamma_{\pm g}$, the $|\psi_+\rangle$ component quickly decays to the ground state, while the $|\psi_-\rangle$ remains for a time $\sim 1/\Gamma_{-g}$. Concurrence $\mathcal{C}_{\max}$ as function of the spacing $\kappa\Delta x$ and time, for giant and small atoms, is shown in Fig. 4(a), with the maximum amount of entanglement $\mathcal{C}_{\max}(\kappa\Delta x) = \max_t \mathcal{C}(\kappa\Delta x, t)$ created by decay for $\kappa\Delta x = 0.99\pi$. The decay dynamics in Fig. 4(b) reveals that concurrence is created at late times. The difference in the entanglement generation comes from the fact that, for small atoms, this entanglement comes from the population of the superradiant mode, whereas for giant atoms the entanglement results from the population in the subradiant mode [30].

Sudden birth of entanglement in giant atoms comes from the unbalanced amount of population in the states $|\psi_\pm\rangle$, which arises from the asymmetry between the decay rates $\Gamma_{e\pm}$ and $\Gamma_{\pm g}$. Since $\Gamma_{e-} \gg \Gamma_{-g}$ and $\Gamma_{e+} < \Gamma_{+g}$ [for the case highlighted in Fig. 4(a)], the atomic population is transferred from $|ee\rangle$ to $|\psi_-\rangle$ faster than from $|\psi_-\rangle$ to $|gg\rangle$, while population decaying from $|ee\rangle$ to $|\psi_+\rangle$ is quickly transferred to $|gg\rangle$. It leads to an efficient generation of entanglement through the control of the waveguide wave number κ. In the Supplemental Material [30], we show that other geometries of giant atoms lead to a sudden birth of entanglement that is comparable to the one for small atoms [Figs. 4(a) and 4(b)].

Giant photon bunching.— We discuss how the statistics of the light emitted by two giant atoms in the waveguide can be used as an entanglement witness of the system. The light emitted by the atoms is described by the electric field operator $\hat{E}_a(t,\vec{r})$ emitted by the atoms. For our system, the left and right traveling fields read [30]

$$\hat{E}^{\mathbf{l}}_a(t) \propto \sum_{n=1}^{N}\sum_{j=1}^{K_n} e^{-ikx_j^{(n)}}\sigma_n^-(t), \qquad \hat{E}^{\mathbf{r}}_a(t) \propto \sum_{n=1}^{N}\sum_{j=1}^{K_n} e^{ikx_j^{(n)}}\sigma_n^-(t), \tag{6}$$

assuming that the phase at a given connection point $x_\ell^{(n)}$ of the atom varies very slowly with the wave number κ.

We characterize the emitted light by its steady-state, second-order correlation function $g^{(2)}(\tau)$ which, for the field $\hat{E}^\alpha_a(t)$ $(\alpha = \{\mathbf{l},\mathbf{r}\})$, is given by

$$g^{(2)}_\alpha(\tau) = \lim_{t\to\infty} \frac{\langle \hat{E}^{\alpha\dagger}_a(t)\hat{E}^{\alpha\dagger}_a(t+\tau)\hat{E}^{\alpha}_a(t+\tau)\hat{E}^{\alpha}_a(t)\rangle}{\langle \hat{E}^{\alpha\dagger}_a(t)\hat{E}^{\alpha}_a(t)\rangle\langle \hat{E}^{\alpha\dagger}_a(t+\tau)\hat{E}^{\alpha}_a(t+\tau)\rangle}. \tag{7}$$

Finally, we define the (steady-state) Mandel Q parameter for the field $\hat{E}^\alpha_a(t,\vec{r})$ as [47]

$$Q_\alpha = \lim_{t\to\infty} \langle \hat{E}^{\alpha\dagger}_a(t)\hat{E}^{\alpha}_a(t)\rangle (g^{(2)}_\alpha(t,t) - 1). \tag{8}$$

By tuning the external field frequency regarding to the atomic transition ω, $\omega_{\text{field}} = \omega - \Delta_p$, the atomic steady state and the emitted light statistics change as shown in Fig. 5. Figures 5(a) and 5(b) show the functions $g^{(2)}_\alpha(0)$ and Q_α, respectively. The light statistics can be changed from sub-Poissonian statistics to superbunching by adjusting the detuning Δ_p in the interval $[-2\Delta_{12}, 2\Delta_{12}]$. While the light statistics of small atoms remain sub-Poissonian, the light emitted from giant atoms exhibit different properties depending on the detuning Δ_p. In particular, giant photon bunching has been reported in a system of quantum dots

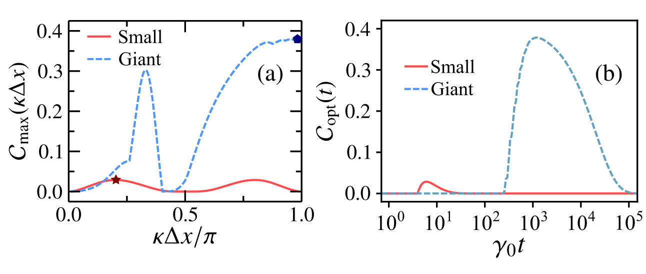

FIG. 4. (a) Maximum amount of entanglement generated through sudden birth for small and giant nested atoms as a function of $\kappa\Delta x$. (b) Dynamics of the optimal sudden birth of entanglement for small and giant nested atoms as a function of $\gamma_0 t$. Here $\kappa\Delta x \approx 0.19\pi$ for small atoms and $\kappa\Delta x = 0.99\pi$ for giant nested atoms.

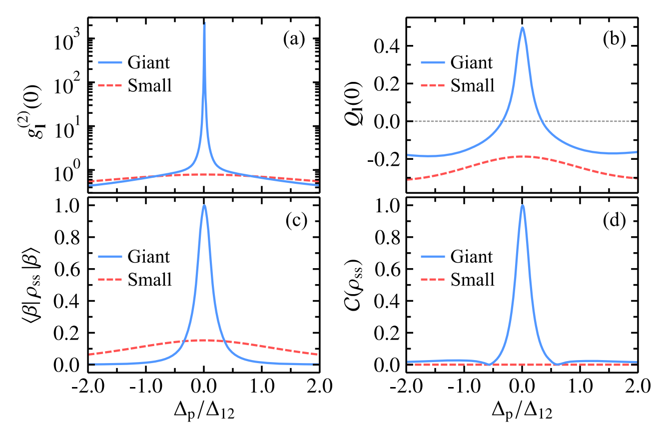

FIG. 5. (a) Function $g^{(2)}_\alpha(0)$ and (b) Mandel parameter for the emitted light by small and giant atoms, as a function of the pumping detuning Δ_p. (c) Population in the state $|\beta\rangle$ and (d) the corresponding concurrence. Here $\Omega_0 = 1.5\gamma_0$ and $\kappa\Delta x = 0.01\pi$.

[48], a system that, in principle, may behave as giant atoms due to the spatial extent of the system, as compared to the pump wavelength [16,49,50].

Figures 5(c) and 5(d) show the entanglement and population of the long-lived state $|\beta\rangle$, respectively. From Fig. 5(c), we observe that when the external pump is at resonance, $\Delta_p \approx 0$, the steady state is $\rho_{\mathrm{SS}}^{\mathrm{nested}} \approx |\beta\rangle\langle\beta|$, such that the entanglement originates due to the large population of the long-lived maximally entangled state $|\beta\rangle$. In this scenario, the behavior of the coherence second-order function and Mandel parameter suggests that these quantities work as a witness of maximally entangled states of the system. Therefore, although bunching of light is not an entanglement witness, in general, the giant bunching observed in the steady-state regime of our dynamics is associated with the generation of long-lived maximally entangled states for two nested giant atoms. In this particular setup, the photon statistics could thus be used to monitor the atomic state.

Conclusion.—Considering two giant atoms driven by photon-mediated interaction and external fields, we have studied entanglement generation. We showed that the phase acquired by the traveling photon inside the waveguide allows us to design a two-qubit system with both frequency-tunable collective decay rates and transition rates between the states of the system. Consequently, frequency-tunable collective effects of two giant atoms are achieved. We have taken advantage of these properties to create a high degree of entanglement in the system through two different processes: free decay and pump-driven dynamics. The amount of concurrence obtained for giant atoms is much larger than for small atoms. In particular, it is possible to create a quasi-maximally-entangled steady state with giant atoms, by adequately adjusting the Rabi frequency of the classical external field that drives the system. Finally, we observe that the statistics of the light emitted in the waveguide are a witness for concurrence generated in the system, so it can be used as a nondestructive measurement for entanglement. By adjusting the external field detuning Δ_p, giant photon bunching emission [48] is observed as the entanglement increases.

Our results can be implemented in superconducting circuits, since the experimental realization of a similar system has been reported by Kannan *et al.* [26]. The two frequency-tunable transmon qubits used in Ref. [26] should be coupled to the transmission line coplanar waveguide at two locations, as shown in Fig. 1(a), instead of the braided manner considered in Ref. [26]. Experimental realization and the immediate extension of our analysis for systems of many giant atoms are left for future prospects.

A. C. S. and R. B. are supported by São Paulo Research Foundation (FAPESP) (Grants No. 2018/15554-5, No. 2019/13143-0, No. 2019/22685-1, and No. 2021/10224-0). R. B. has received support from grants from the National Council for Scientific and Technological Development (CNPq, Grants No. 313886/2020-2 and No. 409946/2018-4). This work has been supported by the French government, through the UCA$^{\mathrm{JEDI}}$ Investments in the Future project managed by the National Research Agency (ANR) with the reference number ANR-15-IDEX-01.

*ac_santos@df.ufscar.br
†romain@ufscar.br

[1] A. Wallraff, D. I. Schuster, A. Blais, L. Frunzio, R.-S. Huang, J. Majer, S. Kumar, S. M. Girvin, and R. J. Schoelkopf, Strong coupling of a single photon to a superconducting qubit using circuit quantum electrodynamics, Nature (London) **431**, 162 (2004).
[2] A. F. van Loo, A. Fedorov, K. Lalumière, B. C. Sanders, A. Blais, and A. Wallraff, Photon-mediated interactions between distant artificial atoms, Science **342**, 1494 (2013).
[3] J. A. Mlynek, A. A. Abdumalikov, C. Eichler, and A. Wallraff, Observation of Dicke superradiance for two artificial atoms in a cavity with high decay rate, Nat. Commun. **5**, 1 (2014).
[4] J.-T. Shen and S. Fan, Strongly Correlated Two-Photon Transport in a One-Dimensional Waveguide Coupled to a Two-Level System, Phys. Rev. Lett. **98**, 153003 (2007).
[5] H. Zheng, D. J. Gauthier, and H. U. Baranger, Strongly correlated photons generated by coupling a three- or four-level system to a waveguide, Phys. Rev. A **85**, 043832 (2012).
[6] Z. Wang *et al.*, Controllable Switching between Superradiant and Subradiant States in a 10-qubit Superconducting Circuit, Phys. Rev. Lett. **124**, 013601 (2020).
[7] D. Gottesman and I. L. Chuang, Demonstrating the viability of universal quantum computation using teleportation and single-qubit operations, Nature (London) **402**, 390 (1999).
[8] L. DiCarlo *et al.*, Demonstration of two-qubit algorithms with a superconducting quantum processor, Nature (London) **460**, 240 (2009).
[9] C. H. Bennett, G. Brassard, C. Crepeau, R. Jozsa, A. Peres, and W. K. Wootters, Teleporting an Unknown Quantum State via Dual Classical and Einstein-Podolsky-Rosen Channels, Phys. Rev. Lett. **70**, 1895 (1993).
[10] J.-G. Ren *et al.*, Ground-to-satellite quantum teleportation, Nature (London) **549**, 70 (2017).
[11] F. Tacchino, A. Auffèves, M. F. Santos, and D. Gerace, Steady State Entanglement beyond Thermal Limits, Phys. Rev. Lett. **120**, 063604 (2018).
[12] Z. Wang, W. Wu, and J. Wang, Steady-state entanglement and coherence of two coupled qubits in equilibrium and nonequilibrium environments, Phys. Rev. A **99**, 042320 (2019).
[13] S. F. Huelga, A. Rivas, and M. B. Plenio, Non-Markovianity-Assisted Steady State Entanglement, Phys. Rev. Lett. **108**, 160402 (2012).
[14] M. H. Oliveira *et al.*, Steady-state entanglement generation for non-degenerate qubits, arXiv:2205.10590.

[15] A. Frisk Kockum, P. Delsing, and G. Johansson, Designing frequency-dependent relaxation rates and Lamb shifts for a giant artificial atom, Phys. Rev. A **90**, 013837 (2014).

[16] A. F. Kockum, in *International Symposium on Mathematics, Quantum Theory, and Cryptography* (Springer, Singapore, 2020), pp. 125–146.

[17] R. Manenti, A. F. Kockum, A. Patterson, T. Behrle, J. Rahamim, G. Tancredi, F. Nori, and P. J. Leek, Circuit quantum acoustodynamics with surface acoustic waves Nat, Nat. Commun. **8**, 975 (2017).

[18] A. Noguchi, R. Yamazaki, Y. Tabuchi, and Y. Nakamura, Qubit-Assisted Transduction for a Detection of Surface Acoustic Waves near the Quantum Limit, Phys. Rev. Lett. **119**, 180505 (2017).

[19] A. N. Bolgar, J. I. Zotova, D. D. Kirichenko, I. S. Besedin, A. V. Semenov, R. S. Shaikhaidarov, and O. V. Astafiev, Quantum Regime of a Two-Dimensional Phonon Cavity, Phys. Rev. Lett. **120**, 223603 (2018).

[20] A. M. Vadiraj, A. Ask, T. G. McConkey, I. Nsanzineza, C. W. Sandbo Chang, A. F. Kockum, and C. M. Wilson, Engineering the level structure of a giant artificial atom in waveguide quantum electrodynamics, Phys. Rev. A **103**, 023710 (2021).

[21] X. Wang, T. Liu, A. F. Kockum, H. R. Li, and F. Nori, Tunable Chiral Bound States with Giant Atoms, Phys. Rev. Lett. **126**, 043602 (2021).

[22] L. Du, Y. Zhang, J. H. Wu, A. F. Kockum, and Y. Li, Giant Atoms in a Synthetic Frequency Dimension, Phys. Rev. Lett. **128**, 223602 (2022).

[23] W. Zhao and Z. Wang, Single-photon scattering and bound states in an atom-waveguide system with two or multiple coupling points, Phys. Rev. A **101**, 053855 (2020).

[24] A. F. Kockum, G. Johansson, and F. Nori, Decoherence-Free Interaction between Giant Atoms in Waveguide Quantum Electrodynamics, Phys. Rev. Lett. **120**, 140404 (2018).

[25] A. Soro and A. F. Kockum, Chiral quantum optics with giant atoms, Phys. Rev. A **105**, 023712 (2022).

[26] B. Kannan *et al.*, Waveguide quantum electrodynamics with superconducting artificial giant atoms, Nature (London) **583**, 775 (2020).

[27] H. Yu, Z. Wang, and J.-H. Wu, Entanglement preparation and nonreciprocal excitation evolution in giant atoms by controllable dissipation and coupling, Phys. Rev. A **104**, 013720 (2021).

[28] R. Barends *et al.*, Superconducting quantum circuits at the surface code threshold for fault tolerance, Nature (London) **508**, 500 (2014).

[29] P. Krantz, M. Kjaergaard, F. Yan, T. P. Orlando, S. Gustavsson, and W. D. Oliver, A quantum engineer's guide to superconducting qubits, Appl. Phys. Rev. **6**, 021318 (2019).

[30] See Supplemental Material at http://link.aps.org/supplemental/10.1103/PhysRevLett.130.053601 for more details about the master equation used to describe the system, for further information of the lifetime discussed in the Letter, and for discussion of superradiant entanglement generation in small atoms, which includes Refs. [31–34].

[31] J. Combes, J. Kerckhoff, and M. Sarovar, The SLH framework for modeling quantum input-output networks, Adv. Phys. **2**, 784 (2017).

[32] J. Gough and M. R. James, The series product and its application to quantum feedforward and feedback networks, IEEE Trans. Autom. Control **54**, 2530 (2009).

[33] P. Azodi, P. Setoodeh, A. Khayatian, and M. H. Asemani, Uncertainty decomposition of quantum networks in SLH framework, Int. J. Robust Nonlinear Control **29**, 6542 (2019).

[34] L. Mandel and E. Wolf, *Optical Coherence and Quantum Optics* (Cambridge University Press, Cambridge, England, 1995).

[35] L. Du, Y.-T. Chen, Y. Zhang, and Y. Li, Giant atoms with time-dependent couplings, Phys. Rev. Res. **4**, 023198 (2022).

[36] X. Wang and H.-R. Li, Chiral quantum network with giant atoms, Quantum Sci. Technol. **7**, 035007 (2022).

[37] L. Du, Y. Zhang, and Y. Li, Giant atoms with modulated transition frequency, Front. Phys. **18**, 12301 (2023).

[38] Q.-Y. Qiu, Y. Wu, and X.-Y. Lü, Collective radiance of giant atoms in non-Markovian regime, Sci. China Phys. Mech. Astron. **66**, 224212 (2023).

[39] X.-L. Yin, W.-B. Luo, and J.-Q. Liao, Non-Markovian disentanglement dynamics in double-giant-atom waveguide-QED systems, Phys. Rev. A **106**, 063703 (2022).

[40] R. H. Dicke, Coherence in spontaneous radiation processes, Phys. Rev. **93**, 99 (1954).

[41] R. Tana and Z. Ficek, Entangling two atoms via spontaneous emission, J. Opt. B **6**, S90 (2004).

[42] A. Cidrim, T. S. doEspiritoSanto, J. Schachenmayer, R. Kaiser, and R. Bachelard, Photon Blockade with Ground-State Neutral Atoms, Phys. Rev. Lett. **125**, 073601 (2020).

[43] L. A. Williamson, M. O. Borgh, and J. Ruostekoski, Superatom Picture of Collective Nonclassical Light Emission and Dipole Blockade in Atom Arrays, Phys. Rev. Lett. **125**, 073602 (2020).

[44] J.-B. Trebbia, Q. Deplano, P. Tamarat, and B. Lounis, Tailoring the superradiant and subradiant nature of two coherently coupled quantum emitters, Nat. Commun. **13**, 1 (2022).

[45] S. A. Hill and W. K. Wootters, Entanglement of a Pair of Quantum Bits, Phys. Rev. Lett. **78**, 5022 (1997).

[46] M. A. Nielsen and I. L. Chuang, *Quantum Computation and Quantum Information: 10th Anniversary Edition*, 10th ed. (Cambridge University Press, New York, NY, 2011).

[47] L. Mandel, Sub-Poissonian photon statistics in resonance fluorescence, Opt. Lett. **4**, 205 (1979).

[48] F. Jahnke *et al.*, Giant photon bunching, superradiant pulse emission and excitation trapping in quantum-dot nanolasers, Nat. Commun. **7**, 1 (2016).

[49] M. Arcari *et al.*, Near-Unity Coupling Efficiency of a Quantum Emitter to a Photonic Crystal Waveguide, Phys. Rev. Lett. **113**, 093603 (2014).

[50] L. Ginés *et al.*, High Extraction Efficiency Source of Photon Pairs Based on a Quantum Dot Embedded in a Broadband Micropillar Cavity, Phys. Rev. Lett. **129**, 033601 (2022).